



Research article

Basalt, glass and carbon fibers and their fiber reinforced polymer composites under thermal and mechanical load

Eduard Kessler^{1,*}, Rainer Gadow², and Jona Straub²

¹ NuCellSys GmbH, Neue Strasse 95, D-73230 Kirchheim u. Teck, Germany

² Institute for Manufacturing Technologies of Ceramic Components and Composites (IFKB), University of Stuttgart, Allmandring 7B, D-70569 Stuttgart, Germany

* **Correspondence:** Email: eduard.kessler@daimler.com; Tel: +49-7021-89-3068.

Abstract: In order to enhance customer acceptance cost optimization is essential regarding future drive trains, like the fuel cell drive. Regarding the pressure vessels, which are needed to store the hydrogen, carbon fibers are the main cost driver. Therefore basalt fibers were identified as a cost effective alternative in previous studies. As fire load is one of the crucial tests in pressure vessel examination, the authors focused on the effect of thermal load on the mechanical properties of basalt fibers and their composites in this work. Therefore tensile tests were performed on impregnated basalt rovings and competing E-glass and carbon rovings after exposition to high temperatures between 100 and 600 °C. Furthermore residual tensile strength of unidirectional basalt-, E-glass-, and carbon reinforced polymers was tested after one-sided thermal load. Both experiments showed that basalt had higher tensile strength at low temperatures or shorter exposition times compared to glass. Yet degradation was more severe and strength was lower at higher temperatures or longer exposition times.

Keywords: polymer matrix composites (PMC); Basalt fibers; Basalt fiber composites; thermomechanical load; filament winding

1. Introduction

According to EU regulation 443/2009 car manufacturers have to reduce CO₂ fleet emissions to 95 g/km until 2020 [1]. Two main strategies for reduction of CO₂ emissions and fleet consumption are lightweight design and alternative drives. In this context natural gas and fuel cell vehicles are promising candidates to reach these goals. For this purpose compressed natural gas (CNG) and compressed hydrogen (CHG) are stored in filament wound high pressure vessels. State of the art, so called type 4 pressure vessels consist of a polymeric liner and metallic bosses, fully reinforced with a carbon-fiber-epoxy composite filament winding [2]. In order to meet challenging cost targets for novel drive trains one focus of current pressure vessel research and development is cost optimization. As carbon fibers stand for at least 70% of pressure vessel cost [3] one possible way is the investigation of alternative reinforcing fibers. In a previous work the authors investigated tensile properties of filament wound unidirectional composites, with a special focus on basalt fibers [4].

One crucial test for pressure vessel certification is the bonfire test. In this test a pressure vessel filled with hydrogen at 70 MPa has to withstand a fire under the whole vessel with a temperature not less than 590 °C for a certain amount of time without rupturing until hydrogen is automatically released through a TPRD (Thermally activated Pressure Relief Device) [5,6]. As this is a very expensive test setup and is only used for final pressure vessel certification, the authors focused on characterization of the reinforcing fibers basalt, E-glass and carbon and their epoxy-composites under thermal and mechanical load on a specimen level at first.

During the last years basalt fibers came into focus of researchers as a cost competitive fiber with slightly higher mechanical properties and thermal and chemical stability than E-glass fibers [7]. As basalt fibers are a natural product, chemical composition and thus fiber properties vary with the mining region [8]. For example high amounts of silicon oxide (SiO₂) and aluminum oxide (Al₂O₃) lead to better mechanical properties [9]. Different oxides affect other properties like thermal and chemical resistance. According to [9] higher amounts of iron oxide lead to a better heat resistance of basalt fibers compared to E-glass fibers [9]. The chemical composition of the investigated basalt fiber is shown in Table 1 [10] and compared to the composition of an E-glass fiber [9].

Table 1. Chemical composition of the investigated basalt fiber [10] and an E-glass fiber [9].

Element Fiber	Na ₂ O [wt%]	MgO [wt%]	Al ₂ O ₃ [wt%]	SiO ₂ [wt%]	K ₂ O [wt%]	CaO [wt%]	TiO ₂ [wt%]	FeO/Fe ₂ O ₃ [wt%]
Basalt	2.8	4.9	19.4	51.8	2.5	7.7	2.1	8.8
E-glass	0.30	0.54	11.86	58.25	0.43	21.09	0.41	0.30

Several works have dealt with thermal load on carbon and glass fibers and their composites, e.g. [11–14], but only a few just recently with thermal load on basalt fibers and their composites [15,16]. Bhat et al. showed that basalt and glass tows show similar quite rapid softening with increasing temperature and time [16]. Yet softening for basalt composite is more severe than for glass composite, residual stresses for basalt are lower at high temperatures. Reason according to [16] is not a more severe softening of the fiber, but a faster heating to higher temperatures of the fiber,

because of higher emissivity. This leads to faster softening and decomposition of the polymer matrix. Jenkins et al. compared residual strength of glass fibers and basalt fibers after thermal load at high temperatures [15]. Having higher tensile strength until about 400 °C, strength of basalt decreases more rapidly over 450 °C, having lower residual strength than glass until 600 °C. Scientific insight is quite low on this topic yet, and the shown two recent works are kind of opposing to the earlier thought that basalt fibers withstand higher temperatures than glass fibers [7,17,18]. Therefore, this study is conducted in order to get more insight on the effect of thermal load on mechanical performance of basalt fibers in comparison to E-glass and carbon fibers. With the gained knowledge of material properties under thermal load pressure vessels with optimized bonfire characteristics shall be designed.

2. Materials and Method

2.1. Materials

Focus in this work was to investigate a commercially available basalt fiber under thermal and mechanical load. Basalt fibers were obtained from ASA.TEC basaltic fibers, Austria and compared to a standard E-glass fiber and the carbon-HT fiber T700 by Toray Industries, which is often used for pressure vessels. Nominal properties of the fibers under investigation are shown in Table 2, as given by the fiber manufacturers. Both basalt and E-glass fibers were provided with a Silan sizing compatible with epoxy matrices. Sizing content of the basalt rovings was 1.0% and 0.7% for the glass fibers respectively. Sizing content was measured by weighing rovings before and after heat treatment at 450 °C for 2 hours.

Table 2. Fibers under investigation and their nominal properties (sources: manufacturer data sheets).

Reinforcing Fiber	Linear density [tex]	Fiber diameter [μm]	Density [g/cm^3]	Tensile strength (manufacturer) [MPa]	Tensile modulus (manufacturer) [GPa]
Basalt	1200	13–20	2.6	2850	90
E-Glass	2400	17	2.45	2450	80
Carbon	800	7	1.8	4900	230

For the impregnation of the rovings as well as for the composite matrix a commercial epoxy resin (type L with hardener EPH161 by PoxySystems, Germany) was used. It is a low viscosity cold-curing resin suitable for filament winding.

2.2. Composite Manufacturing

As described in [4], composite test specimens were manufactured via wet filament winding at the IFKB, University of Stuttgart, Germany. Flat unidirectional composite plates were wound on a square mandrel. Stiffening plates were put on the wound composite in order to create homogeneous

composite plates with plain surfaces. Composite plates with the cold-curing epoxy system cured at room temperature for 24 hours while rotating. Afterwards, the composite plates were removed from the mandrel and put into an oven at 80 °C for 4 hours in order to increase the glass temperature T_G of the plates to about 100 °C.

Composite plates with thicknesses of about $t = 3$ mm were manufactured. Required specimen geometries were cut out with diamond saw blades. Test specimens for tensile testing had the dimensions $250 \times 15 \times t$ mm according to ISO 527-5 specimen type A. On each side 2 mm thick and 50 mm long (± 45) glass-fiber-epoxy cap strips were bonded onto the specimens in order to ensure smooth load transmission and to prevent breaks caused by the fixture jaws. Specimen quality was tested afterwards via reflecting microscopy. Low porosity and a good fiber-matrix bonding were observed. Fiber volume fractions of the tensile test specimens were determined via optical measures at four measuring points for each material. Fiber volume fractions of basalt, glass and carbon composites averaged at 50, 52 and 49%.

2.3. Test Methods

2.3.1. Testing of Rovings

First of all, a thermogravimetric analysis (TGA) in air was performed on short fiber bundles. At a constant heat rate specimens were heated in an oven up to 1200 °C. By measuring mass loss via TGA first conclusions on physical and chemical changes in the test specimen were drawn. For the TGA measurement a Netzsch STA 409 testing device was used.

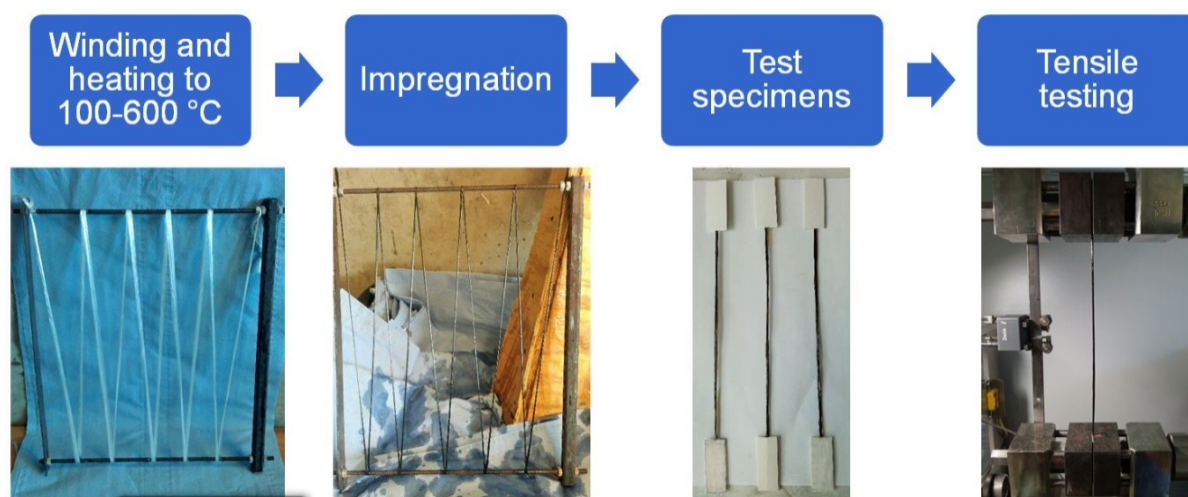


Figure 1. Test procedure including specimen preparation for testing rovings after heat treatment.

In order to provide information on roving properties, tensile tests with impregnated rovings were performed on the basis of German standard DIN 65382 [19], which is close to ASTM D2343. Test procedure is shown in Figure 1. At first, fibers were wound onto a metallic winding rack

without impregnation, opposing to the usual simultaneous impregnation and winding process. These racks were put into an oven for two hours at temperatures between 100 °C and 600 °C in an air environment. After heat treatment and settling to room temperature, the rovings were impregnated manually with the epoxy matrix. As fiber bundles are very brittle after heat exposure, impregnation had to be processed very accurately. 50 mm long cardboard cap strips were bonded onto the ends of the specimens, so that these had a free length of 200 mm. Tensile tests were performed on a Zwick Z100 materials testing machine with a 5 kN load cell at a speed of 1 mm/min. Displacement was measured with a mechanical displacement transducer. At least ten valid tests of each material at each temperature were performed, which means breaking in the free section of the test specimens. The weakening of the fiber due to thermal load is irreversible. Thus a more complex testing with thermal and mechanical load at the same time is not necessary. The chosen test method with fibers cooled down to ambient temperature produces results in good correlation with in-situ measured results [13,16].

2.3.2. Testing of Composite Specimens

Simultaneous flame treatment and tensile testing of flat plates would be ideal to investigate composite materials under thermal and mechanical load. The load case would be similar to that in a bonfire test of pressure vessels. Yet, the necessary kind of equipment is costly and was not available, thermal treatment and mechanical testing were separated. Residual strength of unidirectional composites was tested after a heat treatment of the specimens between one and ten minutes. One-sided heat treatment was performed with a hot air gun, which was regulated to 600 °C and placed 20 mm in front of the specimens in an encapsulated room with an extraction unit. During heat treatment the far side of the heat source was being monitored with an infrared camera by FLIR systems, the front side with a thermocouple to monitor the hot air gun temperature. The heat treatment setup is shown in Figure 2. Afterwards residual tensile strength of polymer fiber composites was tested according to ISO 527-5 [20]. Tensile tests were performed on a Zwick Z100 material testing machine, capable of a maximum force of 100 kN, at a speed of 2 mm/min. Due to availability one to two specimens were tested for each condition.

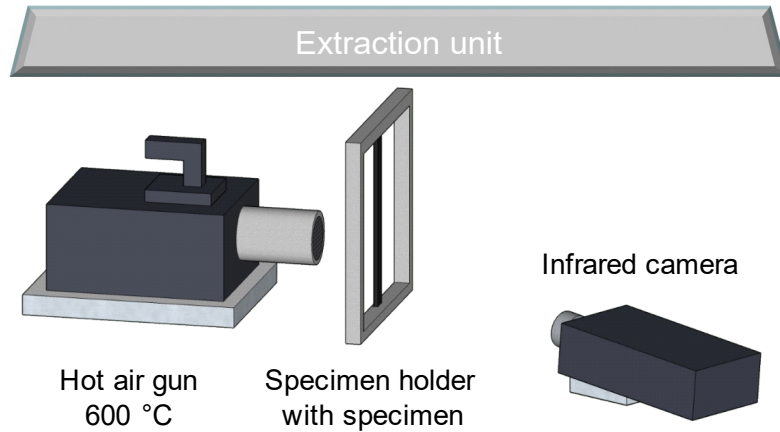


Figure 2. Schematic setup for heat treatment of composite specimens.

3. Results and Discussion

3.1. Roving Specimen

Preliminary to heat and tensile testing of the designated rovings, a thermogravimetric analysis (TGA) was performed in an air environment. Mass loss during thermogravimetric measures of basalt, glass and carbon fibers are shown in Figure 3. For all the fibers a burning of the sizing is visible between about 200 and 400 °C. Sizing content is about 1%. Afterwards mass of basalt and E-glass remains almost constant. Mass loss for basalt is only little higher, which could also be addressed to a higher sizing content. The carbon fiber begins to decompose at about 520 °C. Mass loss continues linearly until about 900 °C, when the fiber is almost completely decomposed and 0.5% of initial mass remains (not shown).

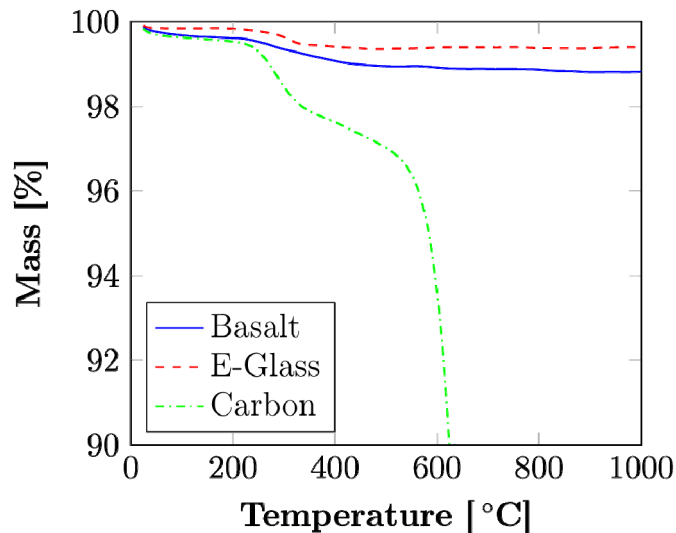


Figure 3. Mass loss of basalt, E-glass and carbon fibers during TGA.

Results of tensile tests on impregnated rovings are shown in Figure 4. Under consideration of the measuring errors, tensile strength of all the tested fibers can be seen as more or less constant until 300 °C. The little decrease of tensile strength at 300 °C might be explained by the removal of the sizing. In a previous work [4], it was shown that the removal of the sizing with Acetone led to a decrease of tensile strength of impregnated basalt rovings of about 7.8%. Between 300 and 400 °C tensile strength of impregnated E-glass and basalt fiber rovings decreases significantly, but for basalt fibers the most, down to almost 40% compared to tensile strength at room temperature, whereas impregnated E-glass rovings still have 60% of their virgin strength. This temperature sensitivity continues until 600 °C, so that E-glass fibers also have higher absolute tensile strength above 300 °C, although the strength value for E-glass fibers at 300 °C in Figure 4 appears as an outlier. For impregnated carbon fiber rovings the biggest decrease in strength appears after 400 °C. This behavior of carbon fibers is confirmed in [21]. Yet carbon fibers are not stable until 600 °C. After heat treatment at 600 °C in air carbon fibers decompose, because of oxidation of the fibers with the oxygen in the air. Further processing is not possible. This finding also confirms the results of the TGA analysis. Although strength of impregnated basalt and E-glass fiber rovings is below that of carbon fiber rovings, also at high temperatures, an advantage of those fibers is that they do not decompose and give a little mechanical resistance and when thinking of fire load on a pressure vessel also heat conduction resistance. As can be seen in Figure 5, tensile modulus remains constant through all temperatures. Tensile modulus of impregnated basalt rovings remains constantly higher than the tensile modulus of E-glass fiber rovings.

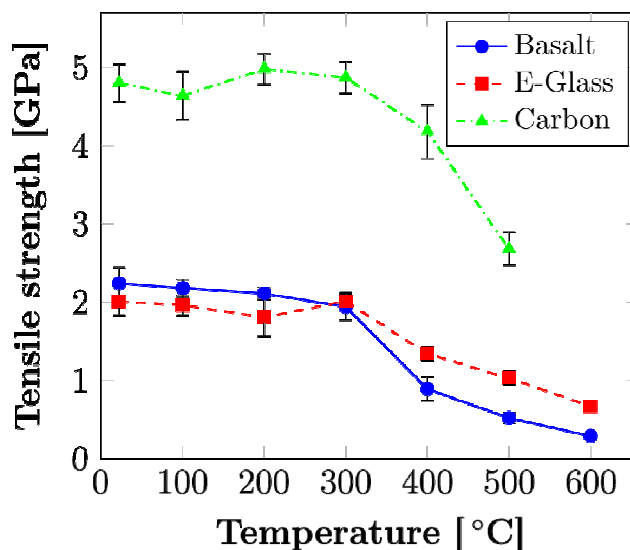


Figure 4. Tensile strength of impregnated basalt, E-glass, and carbon fiber rovings after a two hour heat treatment at temperatures between 100 °C and 600 °C (not visible standard deviations are smaller than data points).

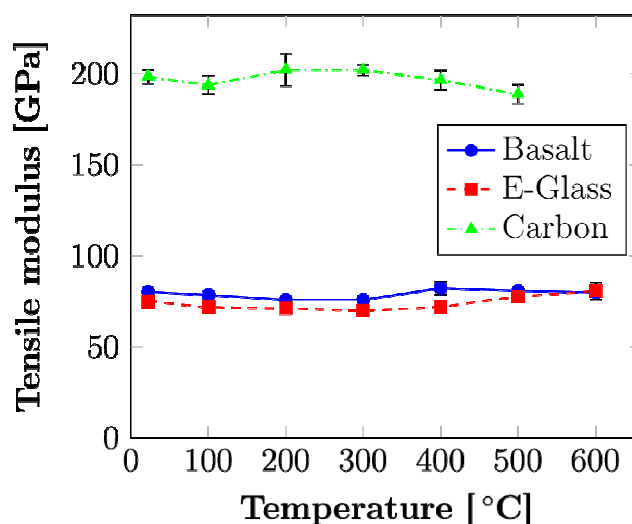


Figure 5. Tensile modulus of impregnated basalt, E-glass, and carbon fiber rovings after a two hour heat treatment at temperatures between 100 °C and 600 °C (not visible standard deviations are smaller than data points).

These obtained results are confirmed by a recent study by Jenkins et al. [15]. Glass and basalt fiber rovings were heat treated for 25 minutes with temperatures up to 600 °C. Single filament tensile tests were performed afterwards. Almost same results were obtained as in this work. At first basalt fibers have a higher tensile strength. At a temperature of about 400 °C tensile strength of basalt fibers decreases below glass fiber values.

Scanning electron micrographs were taken of fracture surfaces of specimens, tested at 100 and 600 °C, respectively 500 °C for carbon rovings, to investigate possible changes in the fibers at high temperatures. For carbon fibers, no change of fracture surfaces could be observed between 100 and 500 °C via SEM. Figure 6 shows fracture surfaces of an impregnated glass fiber roving (a) and basalt roving (b) at 100 °C. Both fracture surfaces look alike, which confirms the glass like properties of basalt fibers. On both SEM pictures a certain amount of fiber pull-out is visible. A typical brittle glass like fracture pattern can be observed for both test specimens, which is described in more detail by Feih et al. [13]. Fracture begins at a near surface defect and progresses through the filament. The starting point can be seen as a smooth surface, the continuation as a shell-like pattern oriented towards the starting point.

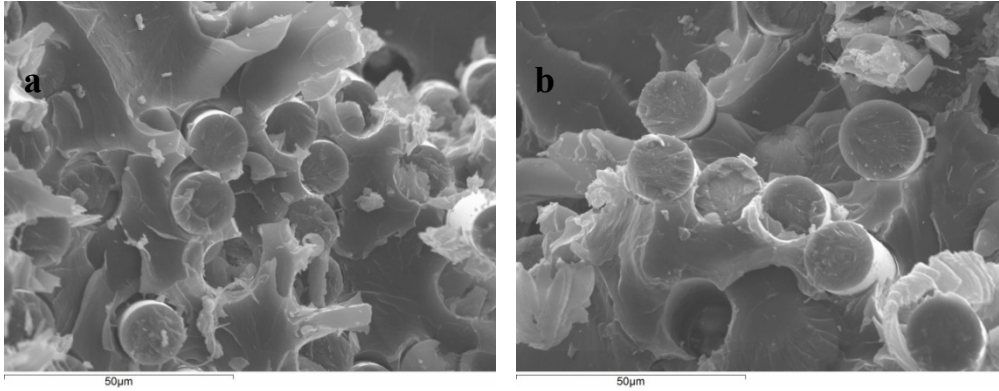


Figure 6. Fracture surfaces of impregnated rovings after heat treatment at 100 °C: (a) E-glass fiber, (b) basalt fiber.

Comparing the fracture surfaces of basalt and glass rovings after heat treatment at 600 °C differences are visible, see Figure 7. Whereas glass fiber fracture remains shell-alike, basalt fiber fracture surface is almost completely flat. Furthermore there is almost no fiber pull-out visible. Not only the filament fracture surface is flat, also the roving fracture is almost on one level. A possible explanation could be the beginning crystallization in the basalt fiber. According to manufacturer's data at a temperature of about 400 °C FeO starts to convert into Fe₂O₃ as well as Fe₂O₃ begins to crystallize [22]. According to Makhova [23] crystallization of basalt fibers begins at temperatures of 500 to 600 °C and the transition is a rapid process for fine fibers. This crystallization leads to a less amorphous structure and consequently to embrittlement. Tensile strength decreases. This finding is contrary to the conclusion from [9], that high amounts of iron oxide in basalt fibers lead to a better thermal stability. High amounts of iron oxide rather enhance the crystallization process.

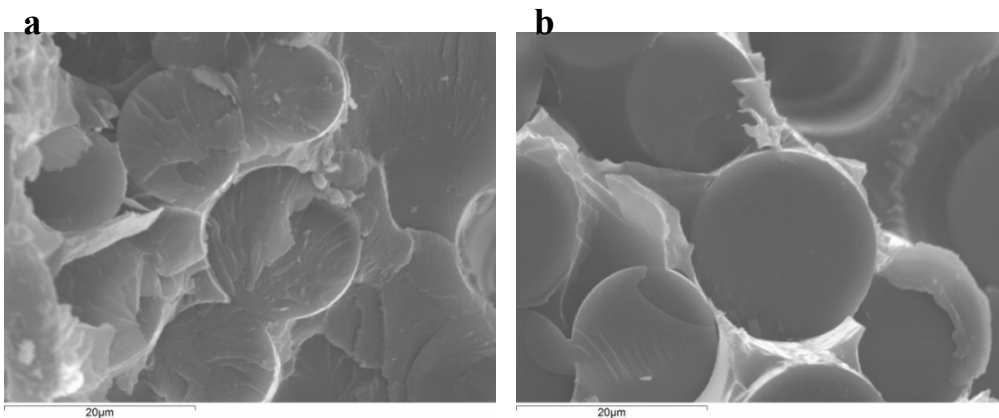


Figure 7. Fracture surfaces of impregnated rovings after heat treatment at 600 °C: (a) E-glass fiber, (b) basalt fiber.

In order to support this assumption polished surfaces of basalt fiber bundles after heat treatment at 100 °C and 600 °C were examined via light and polarization microscopy. Figure 8 shows light microscope images after heat treatment at 100 °C (a) and 600 °C (b). Despite identical specimen preparation the 600 °C specimen shows many defects at filament edges compared to the 100 °C

reference specimen. This is a first sign for brittle fiber behavior due to beginning crystallization. Furthermore the contrast between fiber and matrix is increased compared to the reference specimen. So light refraction has changed, which is another sign for transformation of the fiber structure.

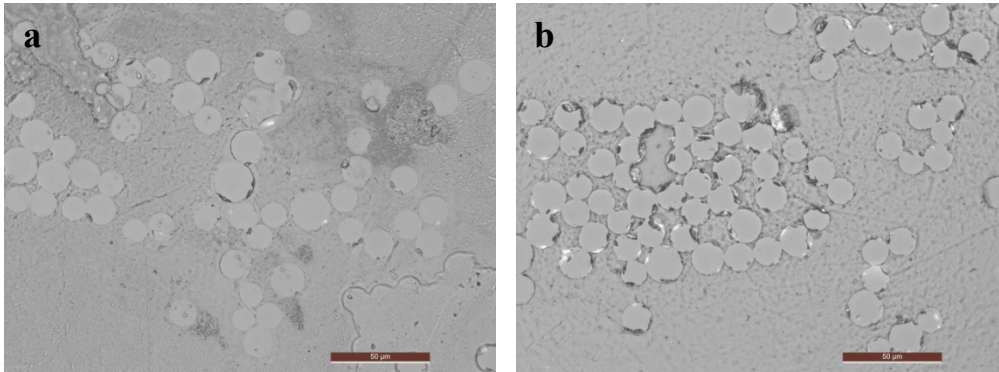


Figure 8. Light microscopy of polished sections of impregnated basalt rovings after heat treatment at (a) 100 °C and (b) 600 °C.

Figure 9 shows polarization microscope images of the polished sections shown in Figure 8. Glass and basalt fibers are amorphous in their original form. In Figure 9a, this can be confirmed for the reference specimen, as all filaments have almost the same dark grey scale, which can hardly be separated from the matrix. The polarized light beam is being refracted identically everywhere. Only filament edges seem to be brightened a little as a result of strain due to fiber-matrix bonding and specimen preparation. Filaments in the 600 °C specimen are considerably brighter than in the reference specimen, the effect of double refraction is visible. Due to beginning crystallization light is being refracted differently and not equally in every direction. Especially filament edges are brightened quite equally. Rearrangement and crystallization seem to begin at filament edges and spread into the filament core. With the optical measures beginning crystallization cannot be quantified, yet it can be visualized.

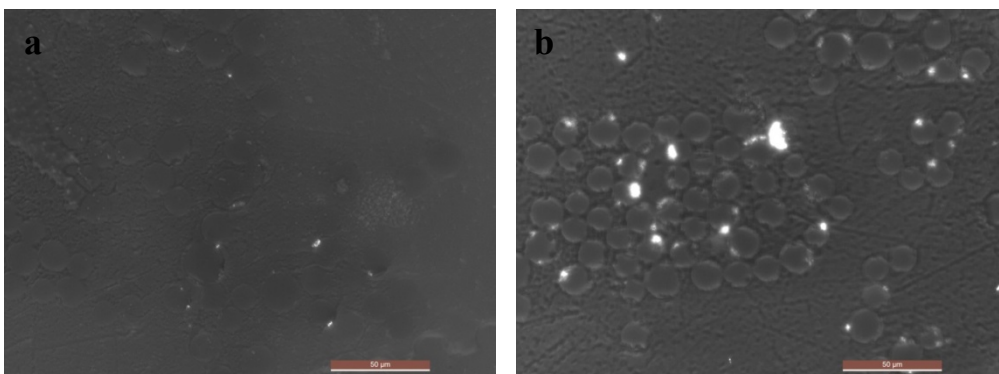


Figure 9. Polarization microscopy of impregnated basalt fiber rovings after heat treatment at (a) 100 °C and (b) 600 °C. Brightening of the 600 °C specimen due to changed light refraction due to beginning crystallization is visible.

3.2. Composite Specimens

During heat treatment of the composite specimens decomposition temperature of the epoxy matrix is exceeded widely. At a constant temperature the amount of decomposed matrix depends on heating time and thermal properties of the composite, especially its thermal conductivity. The heat effect is qualitatively the same for all tested fiber reinforced polymers. Therefore the glass fiber composite specimens are shown in the following, due to better visibility, see Figure 10. After a few seconds a black coloring of the composite was visible, which results from an unfinished decomposition of the matrix. After about three minutes, first fibers became visible in the middle of the heating zone, because of final decomposition of the matrix in this area. With increasing time this area increased. The expansion of decomposition in thickness direction is of special interest, as it influences residual tensile strength the most. As can be seen in Figure 10b, decomposition in thickness direction increased with increasing time, more and more pure fibers as well as delamination in the composite are visible. Furthermore in this side view a bulging of the specimens can be seen, which consists of soot and carbon, decomposed out of the matrix. Basalt and glass fibers remained intact, when matrix was decomposed completely. On the other hand single carbon filaments and larger fiber bundles cracked just due to heat treatment for longer durations. This is a consistent result with regard to previously shown TGA and roving analyses. At about 600 °C in an air environment carbon fibers decompose, also in this composite experimental setup.

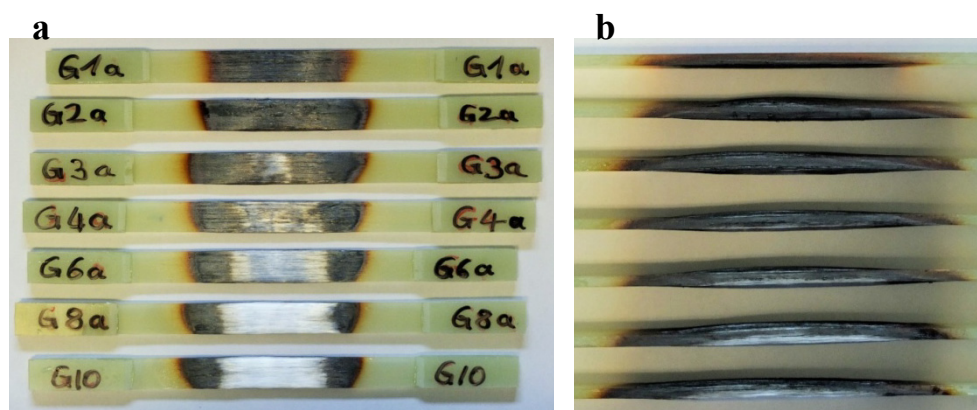


Figure 10. Glass fiber polymer composites after one-sided local heat treatment at 600 °C from one to ten minutes: (a) top view, (b) side view (numbers show time of heat treatment in minutes).

After heat treatment residual tensile strength tests were performed. Results, shown in Figure 11, were similar to roving tests, shown in Figure 4. Even after a short duration tensile strength decreased significantly. Tensile strength of E-glass composites decreased least compared to their virgin strength at room temperature. Tensile strength of basalt composites decreased faster. There was the tendency that after about two minutes tensile strength decreased below the value of E-glass composites. Tensile strength of basalt and carbon composites decreased almost parallel.

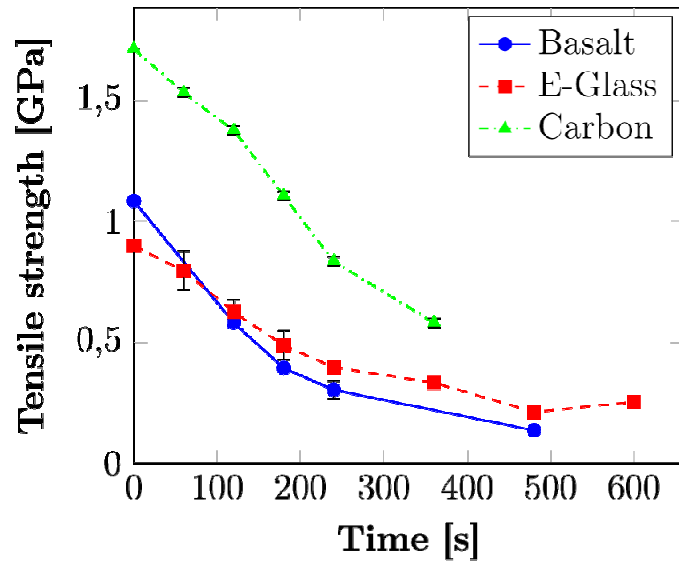


Figure 11. Tensile strength of basalt, E-glass, and carbon fiber polymer composites after one-sided heat treatment at 600 °C between 60 and 600 seconds

Bhat et al. [16] attributed the worse performance of basalt fiber composites compared to glass fiber composites to more distinct matrix softening and decomposition due to higher emissivity and hence temperature because of the basalt fiber. Especially at long durations matrix is decomposed almost completely and strength mostly depends on fiber properties. Yet the glass fiber composite shows a better performance than the basalt fiber composite. This result is supported by infrared camera results in the present investigation. Figure 12 shows the temperature profile of the far side of the heat treated composite specimens measured via infrared camera. It is visible that temperature of basalt specimens was higher compared to the other composites, which probably explains the more severe degradation compared to the glass composite. The carbon composite surface remains below the other two composite materials. Reason is the higher thermal conductivity, which leads to a faster heat conduction to the outer regions of the test specimen, see Figure 13.

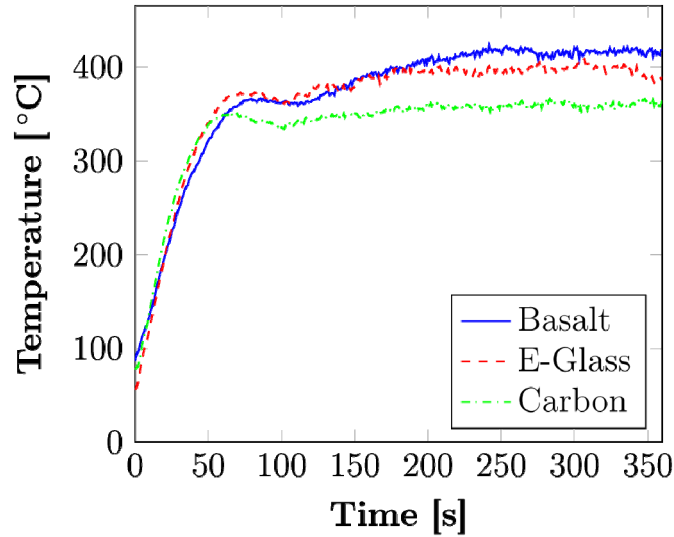


Figure 12. Temperature profile on the far side of composite specimens during heat treatment for basalt-, E-glass- and carbon-epoxy composites recorded by an infrared camera.

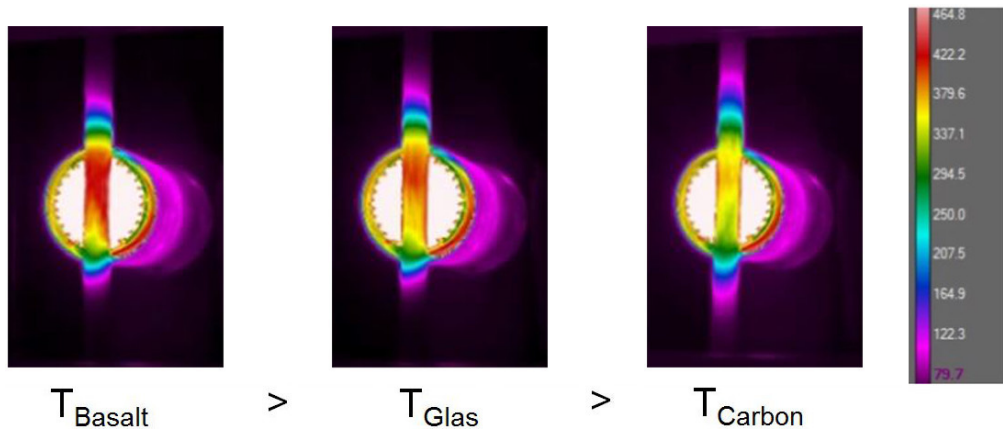


Figure 13. Infrared pictures of basalt, E-glass and carbon composite specimens during heat treatment after 360 seconds.

In order to support this result, temperature conductivity was measured via laser flash analysis with a Netzsch Nanoflash LFA 447 test equipment in thickness and in fiber direction. Combined with measurement of specific heat capacity via differential scanning calorimetry (DSC) and density via Archimedes' principle thermal conductivity λ was determined for basalt-, E-glass and carbon-epoxy composites at room temperature and 200 °C. Results for thermal conductivity are shown in Table 3. Results show a thermal conductivity in fiber direction about 8 to 11 times higher for carbon-epoxy than for basalt-, and E-glass-epoxy, which explains the higher influence zone and lower temperatures for the carbon-epoxy-specimens. At 200 °C the basalt composite has about 20% higher thermal conductivity in thickness direction and 27% lower thermal conductivity in fiber direction

than the glass composite, yet still on a very low level. This supports the result of higher temperatures on the far side of the specimen with a smaller thermal influence zone to some degree.

Summing up the presented results, it can be stated that basalt fibers and basalt-epoxy composites were more sensitive to thermal load than glass fibers and glass-epoxy-composites.

Table 3. Thermal conductivity at 23 °C and 200 °C for basalt-, E-glass- and carbon composites in thickness and in fiber direction.

	λ at 23 °C in W/mK		λ at 200 °C in W/mK	
	Thickness dir.	Fiber dir.	Thickness dir.	Fiber dir.
Basalt	0.59	0.65	0.67	0.72
E-Glass	0.52	0.85	0.56	0.99
Carbon	0.75	5.95	0.95	8.27

With regard to the investigation of basalt fibers as a relatively new reinforcing fiber for polymer matrix composites new insights on the thermal response could be gathered in this work. Basalt fibers show higher mechanical properties compared to glass fibers at low temperatures, yet they show a more severe softening at higher temperatures or a longer period of thermal load. These findings are contrary to the former viewpoint in the literature. It could be shown that a crystallization process begins in the basalt fibers, which is not visible in glass fibers, at least in this temperature range. Carbon fibers show much higher mechanical properties compared to glass and basalt fibers up to 500 °C. Yet in contrast to these fibers, they break and decompose at higher temperatures.

After the fundamental research shown in this work these findings will be adapted to composite pressure vessels. In combination with a hybrid approach, which was investigated in [23], pressure vessels reinforced by both carbon and basalt fibers will be manufactured to combine both high mechanical strength of carbon fibers and high maximum temperature of basalt fibers and investigate those pressure vessels in a bonfire test. The bonfire test contains temperatures over 600 and 800 °C for different time periods. Therefore basalt fibers on the outside will lead to a longer heat resistance while carbon fibers on the inside will provide the required strength for the high pressure.

4. Conclusion

Different reinforcing fibers and their composites were tested under thermal and mechanical load. Tensile tests on rovings after exposition to high temperatures between 100 and 600 °C showed that basalt fibers had higher initial strength at low temperatures than E-glass fibers. Yet, softening was more severe for basalt fibers and over 300 °C tensile strength of basalt fibers was below of that of glass fibers. SEM showed changed fracture surfaces at high temperatures for basalt fibers, but not for glass fibers. This was assumed to originate from beginning crystallization in the basalt fibers, which was shown via polarization microscopy. Tensile strength of carbon fibers remained constant until about 300 °C and then decreased rapidly until 500 °C. A temperature of 600 °C led to oxidation and hence decomposition of carbon fibers. Tensile modulus remained constant for all fiber materials at all temperatures. Heat treatment and tensile strength measurement of unidirectional composite plates

showed similar results. Again basalt composites had higher initial strength than glass composites, yet softened more severely, so that at high temperatures glass composites had higher residual strength. In conclusion it has to be stated that in contrast to former view basalt fibers and basalt-epoxy composites seem to have lower thermal resistance than glass fibers and glass-epoxy composites. Compared to carbon fibers basalt and glass fibers withstand higher maximum temperatures without decomposition, which can be considered favorable for use for composite pressure vessels.

Conflict of Interest

All authors declare no conflicts of interest in this paper.

References

1. Regulation (EC) no. 443/2009 of the European Parliament and of the Council. *Off J Eur Union*.
2. Mori D, Hirose K (2009) Recent challenges of hydrogen storage technologies for fuel cell vehicles. *Int J Hydrogen Energy* 34: 4569–4574.
3. Hua TQ, Ahluwalia RK, Peng JK, et al. (2011) Technical assessment of compressed hydrogen storage tank systems for automotive applications. *Int J Hydrogen Energy* 36: 3037–3049.
4. Kessler E, Gadow R, Weichand P (2015) Investigation of mechanical properties of filament wound unidirectional basalt fiber reinforced polymers for automotive and pressure vessel application. ICCM 20, 20th International Conference on Composite Materials, Copenhagen, Denmark.
5. Gambone LR, Wong JY (2007) Fire protection strategy for compressed hydrogen-powered vehicles. 2nd International Conference on Hydrogen Safety, San Sebastian, Spain.
6. Ruban S, Heudier L, Jamois D, et al. (2012) Fire risk on high-pressure full composite cylinders for automotive applications. *Int J Hydrogen Energy* 37: 17630–17638.
7. Artemenko SE (2003) Polymer composite materials made from carbon, basalt and glass fibres. Structure and properties. *Fibre Chem* 35: 226–229.
8. Subramanian RV, Austin HF (1980) Silane coupling agents in basalt-reinforced polyester composites. *Int J Adhes Adhes* 1: 50–54.
9. Deak T, Czigany T (2009) Chemical composition and mechanical properties of basalt and glass fibers: a comparison. *Text Res J* 79: 645–651.
10. Gadow R, Weichand P (2014) Novel intermediate temperature ceramic composites, materials and processing for siloxane based basalt fiber composites. *Key Eng Mater* 611: 382–390.
11. Yin Y, Binner JGP, Cross TE, et al. (1994) The oxidation behaviour of carbon fibres. *J Mater Sci* 29: 2250–2254.
12. Feih S, Mouritz AP, Mathys Z, et al. (2007) Tensile strength modeling of glass fiber-polymer composites in fire. *J Compos Mater* 41: 2387–2410.
13. Feih S, Manatpon K, Mathys Z, et al. (2009) Strength degradation of glass fibers at high temperatures. *J Mater Sci* 44: 392–400.
14. Feih S, Boiocchi E, Kandare E, et al. (2009) Strength degradation of glass and carbon fibres at high temperature. ICCM 17, 17th International Conference on Composite Materials, Edinburgh,

Scotland.

15. Jenkins PG, Riopedre-Méndez S, Sáez-Rodríguez E, et al. (2015) Investigation of the strength of thermally conditioned basalt and E-glass fibres. ICCM 20, 20th International Conference on Composite Materials, Copenhagen, Denmark.
16. Bhat T, Chevali V, Liu X, et al. (2015) Fire structural resistance of basalt fibre composite. *Compos Part A-Appl S* 71: 107–115.
17. Morozov NN, Bakunov VS, Morozov EN, et al. (2001) Materials based on basalts from the European north of Russia. *Glass Ceram* 58: 100–104.
18. Sim J, Park C, Moon DY (2005) Characteristics of basalt fiber as a strengthening material for concrete structures. *Compos Part B-Eng* 36: 504–512.
19. German Institute for Standardization DIN 65 382 (1988) Aerospace; Reinforcement fibers for plastics; Tensile test of impregnated yarn test specimens.
20. International Organization for Standardization ISO 527-5 (2010) Plastics—Determination of tensile properties. Part 5: Test conditions for unidirectional fibre-reinforced plastic composites.
21. Feih S, Mouritz AP (2012) Tensile properties of carbon fibres and carbon fibre-polymer composites in fire. *Compos Part A-Appl S* 43: 765–772.
22. Incotology GmbH (2015) Basalt rovings technical data sheet.
23. Makhova MF (1968) Crystallization of basalt fibers. *Glass Ceram* 25: 672–674.
24. Kessler E, Gadow R, Semmler C (2016) Apparent hoop tensile strength of basalt fiber and hybrid fiber reinforced polymers. Proceedings SAMPE Technical Conference, Long Beach, USA.



AIMS Press

© 2016 Eduard Kessler, et al., licensee AIMS Press. This is an open access article distributed under the terms of the Creative Commons Attribution License (<http://creativecommons.org/licenses/by/4.0>)